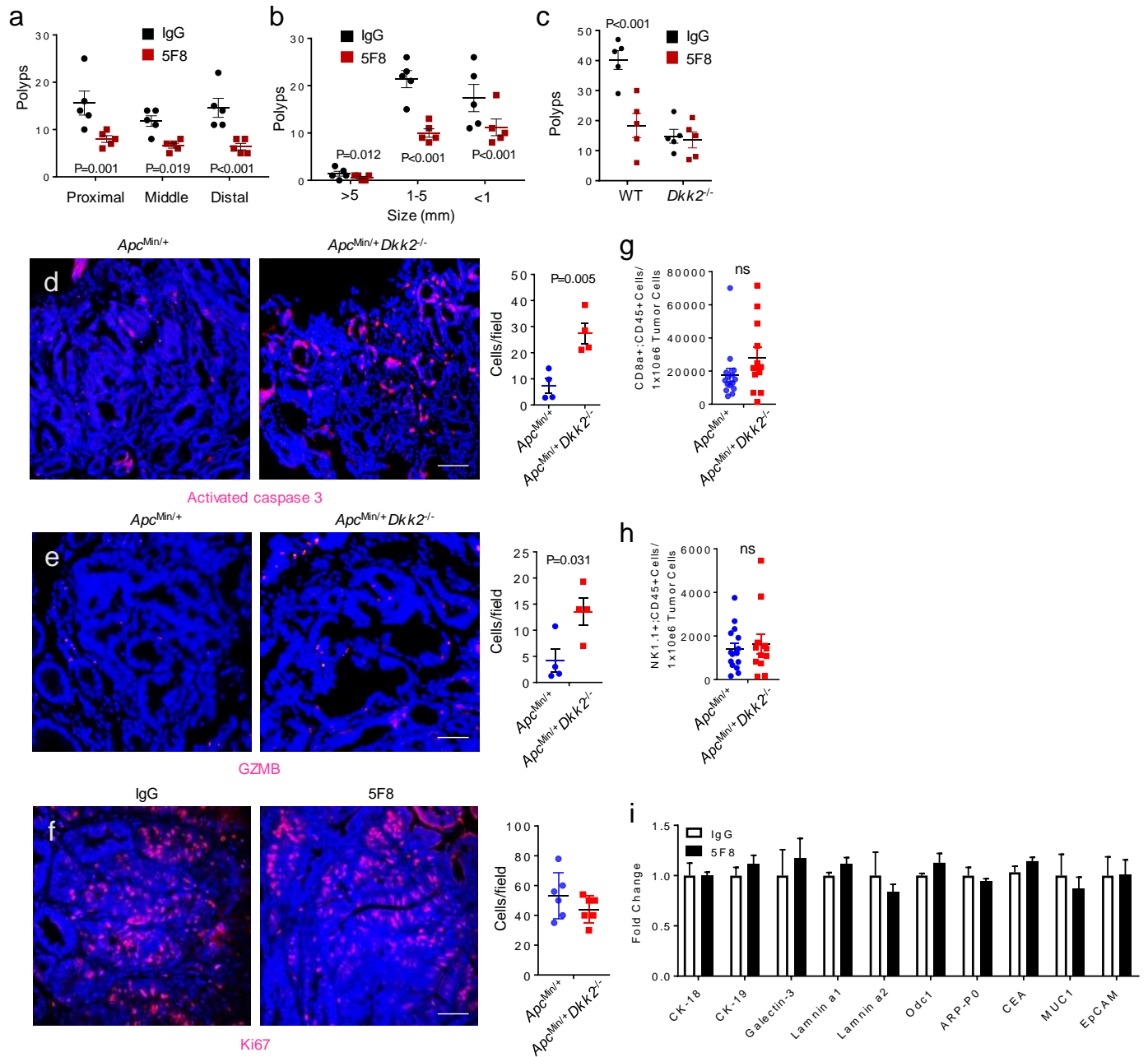
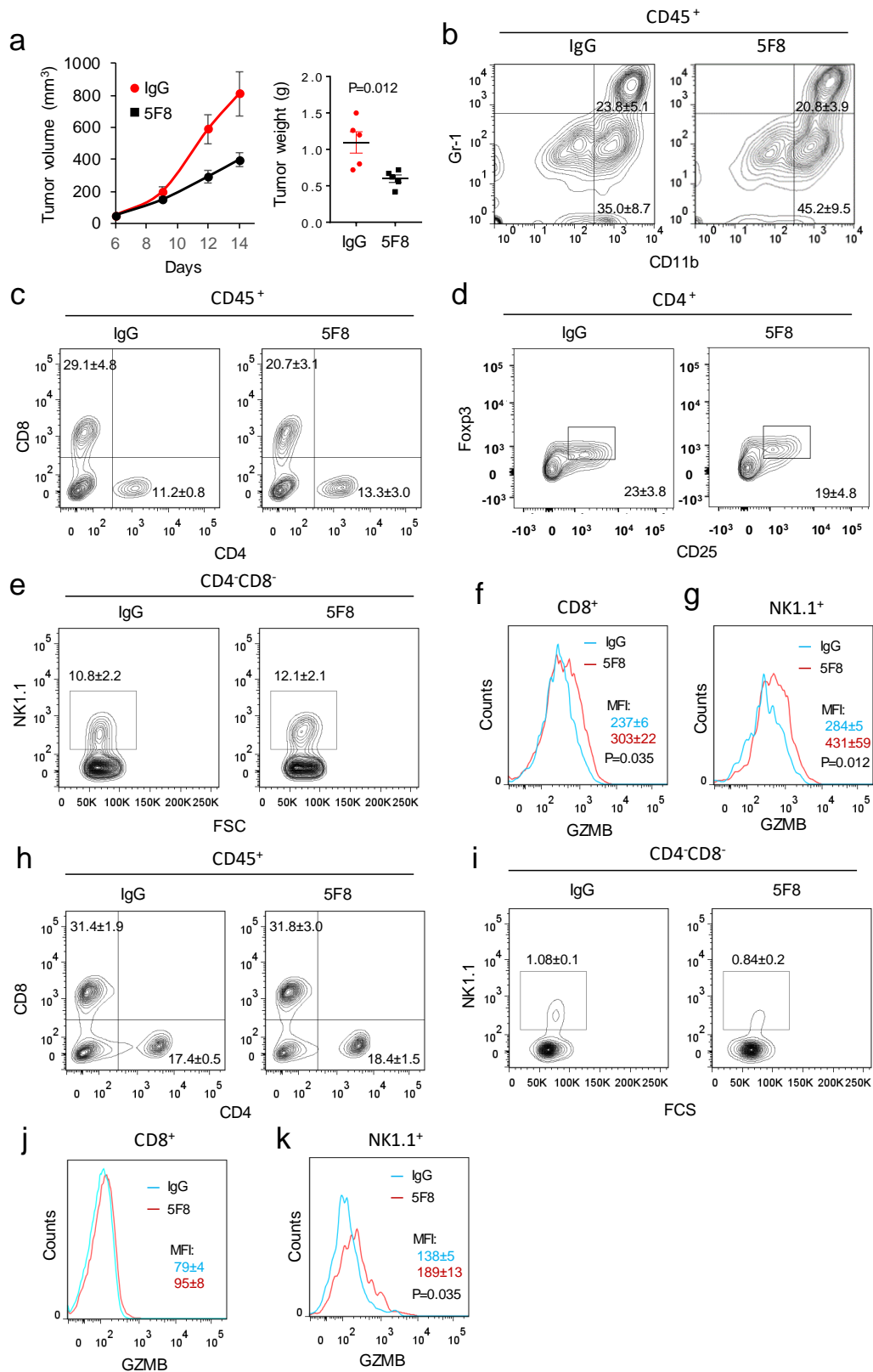


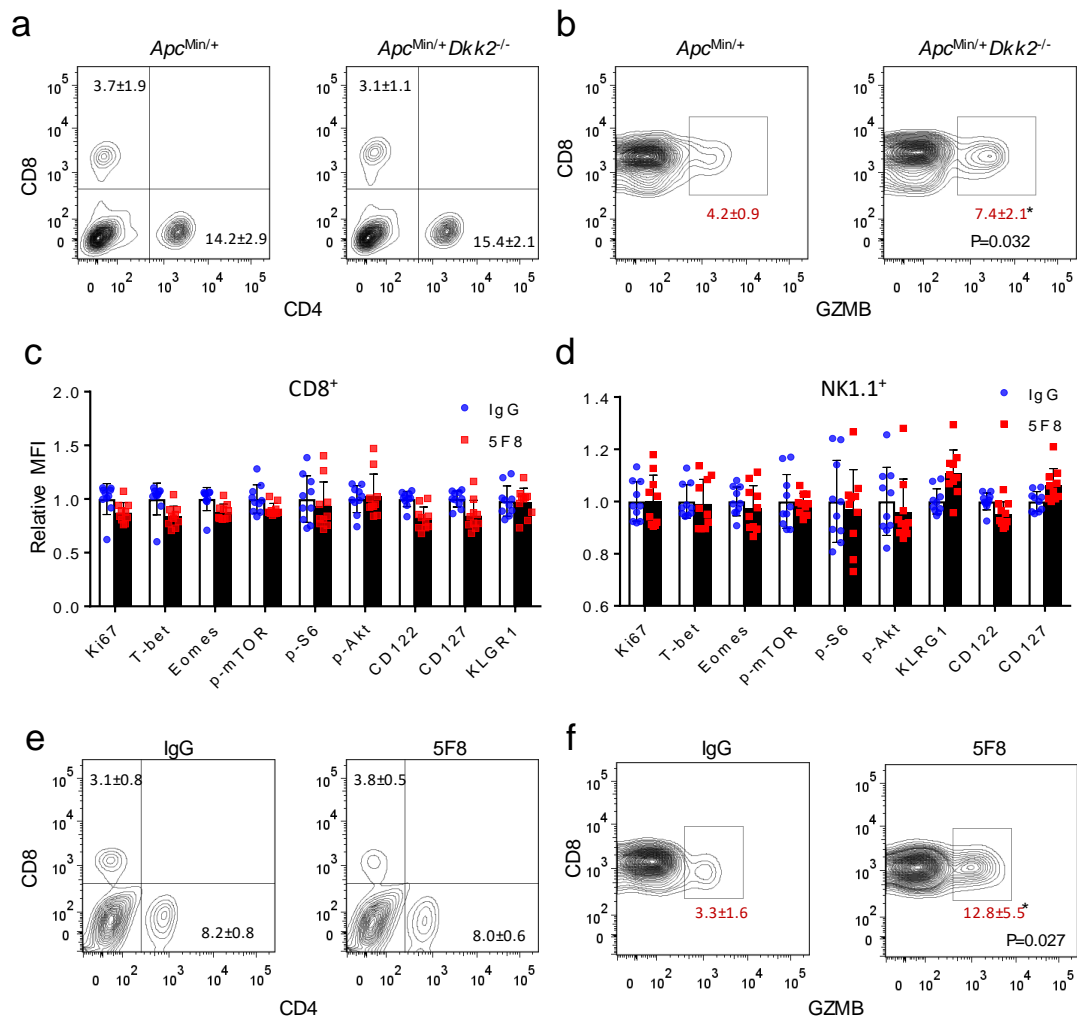
Supplementary Figure 1. Upregulation of DKK2 expression by APC-loss. (a) Upregulation of DKK2 expression in human CRC samples over normal colorectal samples and in MSS CRCs over MSI CRCs. The numbers in the chart denote the sample sizes. (b-d) Upregulation of DKK2 expression in mouse intestinal polyps. DKK2 mRNA levels isolated from polyps and normal intestines from 4 *Apc*^{Min/+} and normal mice, respectively, were determined by quantitative RT-PCR (data are presented as means \pm sem; Two-sided Student t-test, n=4) (b), whereas the DKK2 mRNA (c) and protein (d) in intestinal sections was detected by *in situ* hybridization and Immunostaining, respectively. The sections were processed and exposed simultaneously, and the immunostaining intensity was quantified by ImageJ software. Five independent sections per mouse with 5 mice per group were quantified. Data are presented as means \pm sem (two-sided Student t-test). Red signals are *Dkk2* mRNA, whereas blue signals are nuclear counter stain in c. (e,f) Upregulation of DKK2 expression in APC-loss MC38 cells. DKK2 expression was determined by quantitative RT-PCR (data are presented as means \pm sem; two-sided Student t-test, n=4) using RNAs isolated from MC38 cells with or without the APC mutation (e) or from APC mutant MC38 cells transfected with different β -catenin siRNAs (f). Western analysis of β -catenin levels is also shown. (g) Upregulation of DKK2 expression in APC-loss HCT116 human colon cancer cells. DKK2 expression was determined by quantitative RT-PCR. Data are presented as means \pm sem (Two-sided Student t-test, n=4). (h) Correlation between DKK2 expression and CRC patient survival rates. The overall and relapse-free survival rates of the high (top 15 percentile) and low (bottom 15 percentile) DKK2 expressers are compared using the TCGA provisional datasets of colorectal adenocarcinoma ($P = 0.031$, n=56 for overall survival; $P = 0.036$, n=50 for relapse-free survival) by the two-sided Mantel-Cox Log-Rank test. (i) Verification of the lack of DKK2 protein in DKK2-null mice. Polyps from *Apc*^{Min/+} (DKK2 WT) and *Apc*^{Min/+}*Dkk2*^{-/-} mice were analyzed by Western blotting using the anti-DKK2 antibody. The experiments were repeated twice.



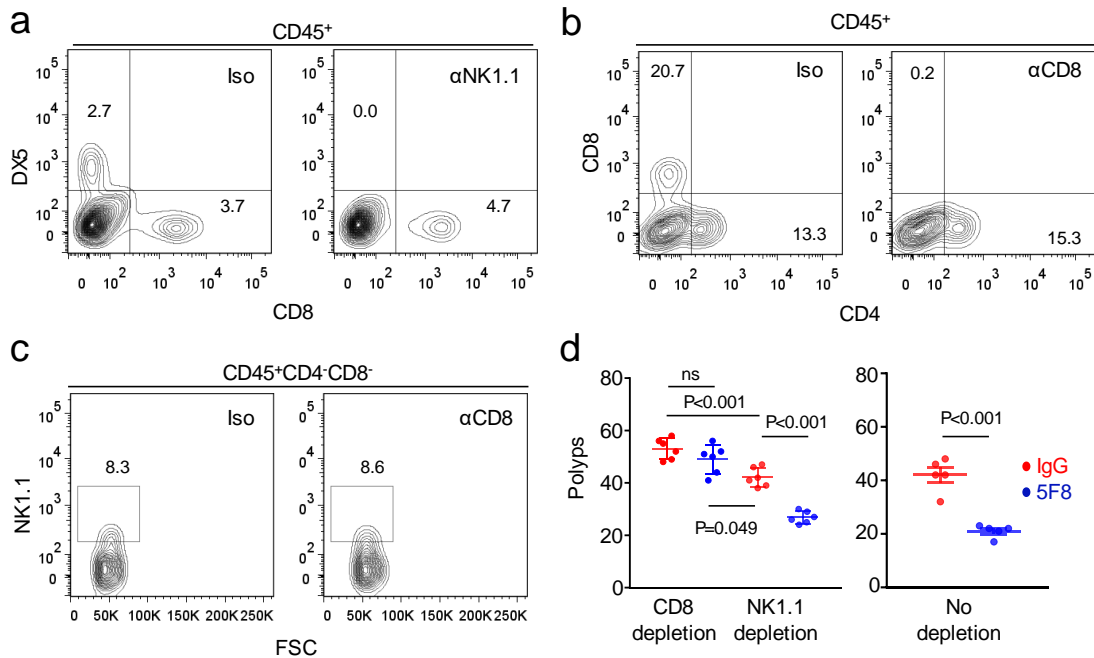
Supplementary Figure 2. Effects of DKK2 blockade on the polyps of the *Apc*^{Min/+} mice. (a,b) The anti-DKK2 antibody reduces tumor burdens in *Apc*^{Min/+} mice. Mice (16 weeks old male) were treated with 5F8 and an isotype antibody (IgG3) (10 mg/kg, once a week, i.p.) for 4 weeks. Polyps numbers in small intestines were counted. Data are presented as means±sem (IgG vs 5F8; n=5; two-way Anova). (c) The effect of 5F8 on tumor suppression depends on DKK2. *Apc*^{Min/+} and *Apc*^{Min/+} *DKK2*^{-/-} mice (10 weeks old female) were treated with 5F8 and an isotype antibody (IgG3) (8 mg/kg, twice a week, i.p.) for 6 weeks. Polyps numbers in small intestines were counted under a stereomicroscope after staining with methylene-blue. Data are presented as means±sem (5F8 vs IgG treated; n=5; two-way Anova). (d-f) DKK2-deficiency increases apoptosis and granzyme B-positive cells without affecting proliferation in the polyps of the *Apc*^{Min/+} mice. Histological sections of polyps collected from the *Apc*^{Min/+} and *Apc*^{Min/+} *Dkk2*^{-/-} mice (20 weeks old) were stained with anti-activated caspase 3, granzyme B or Ki67 antibody together with DAPI. Scale bars are 150 μm. Five independent sections per mouse were quantified from five mice per genotype. Data are presented as means±sem (Two-sided Student t-test). (g-h) Quantification of the numbers of infiltrated CD8⁺ and NK1.1⁺ cells in intestine tumors from *Apc*^{Min/+} and *Apc*^{Min/+} *DKK2*^{-/-} mice based on flow cytometry analysis of dissected polyps. Five large polyps per mouse (20 weeks old) were collected and analyzed by flow cytometry after staining with CD45, CD8⁺, and NK1.1⁺. Data are presented as means±sem (ns, not significant; n=5; Two-sided Student t-test). (i) DKK2 blockade does not affect differentiation in the polyps. Relative expression of a number of intestinal epithelial cell stem and differentiation markers in the polyps dissected from IgG or 5F8 treated *Apc*^{Min/+} mice were examined by quantitative RT-PCR and normalized against the mRNA levels of GAPDH. Data are presented as means±sem (n=5; Two-sided Student t-test).



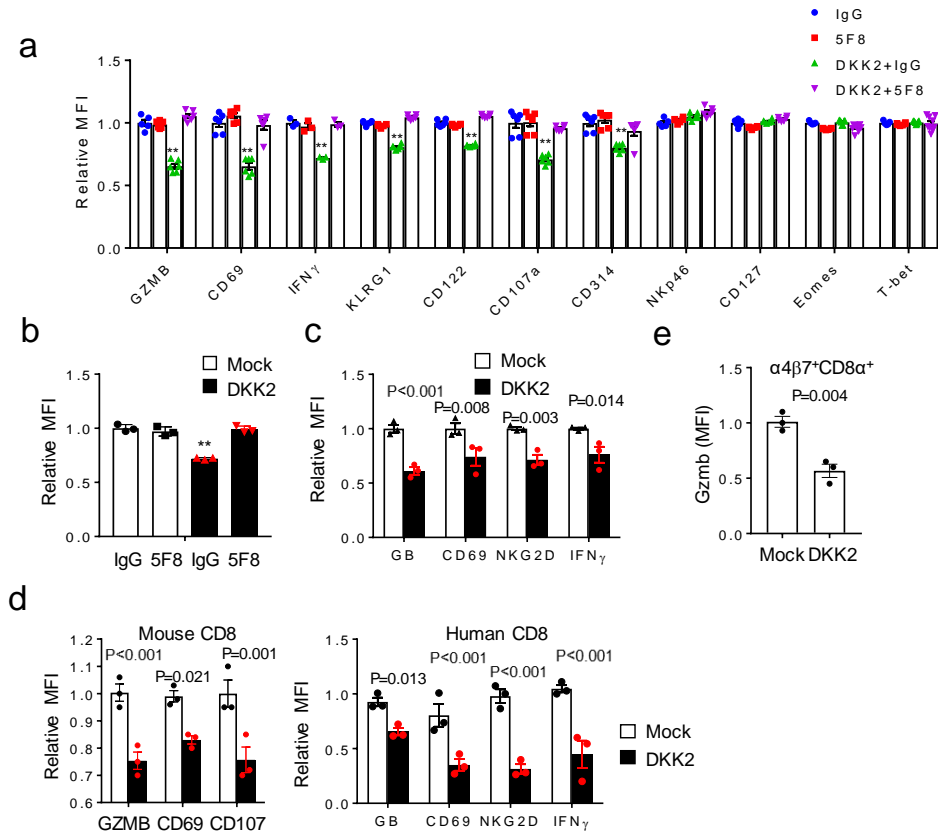
Supplementary Figure 3. Flow cytometry analysis of leukocytes in tumors or lymph nodes. (a-g) Flow cytometry analysis of tumor infiltrated leukocytes. C57BL/6 mice were inoculated s.c. with the MC38 cells. Treatment of 5F8 (10 mg/kg, every three days, i.p.) commenced at Days 9 and 12. Tumors were collected at Day 14 and analyzed by flow cytometry. Panels **d-f** are derived from Panel **c**, whereas Panel **g** is derived from **e**. Data for tumor growth (P=0.034 and 0.024 for Days 12 and 14, respectively; two-way Anova) and weight (two-sided Student's t-test) are presented as means±sem (n=5). **(h-k)** Flow cytometry analysis of tumor draining lymph nodes. Inguinal lymph nodes were collected from mice described above and analyzed by flow cytometry. Data are presented as means±sem (n=5; Two-sided Student's t-test).



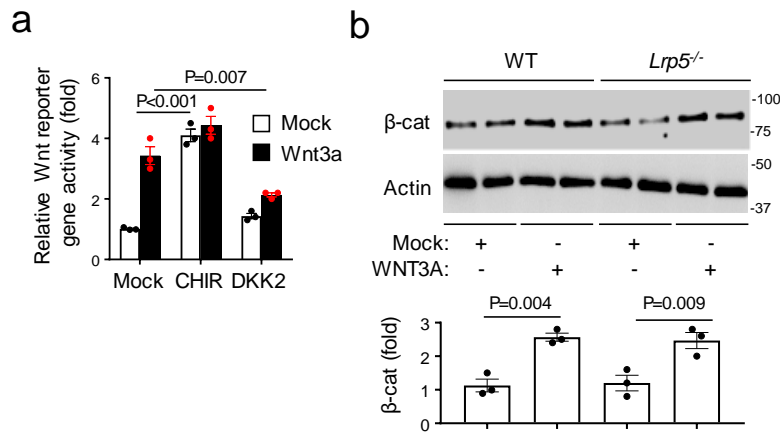
Supplementary Figure 4. Effects of DKK2 blockade on immune effector cell activation. (a,b,e,f) Flow cytometry analysis of leukocytes in Peyer's patches (PPs) of *Apc^{Min/+}* mice. Leukocytes from PP of *Apc^{Min/+}* or *Apc^{Min/+}Dkk2^{-/-}* mice (20 weeks old) (**a,b**) or from *Apc^{Min/+}* mice injected with one dose of 5F8 (10 mg/Kg, i.p.) for 24 hours (**e,f**) were prepared and analyzed by flow cytometry. The populations shown were pre-gated for CD45. Data are presented as means±sem (Two sided Student's t-test; n=5). (**c,d**) Flow cytometry analysis of additional markers of tumor infiltrated CD8⁺ and NK1.1⁺ cells described in Fig. 3g-h (n=10).



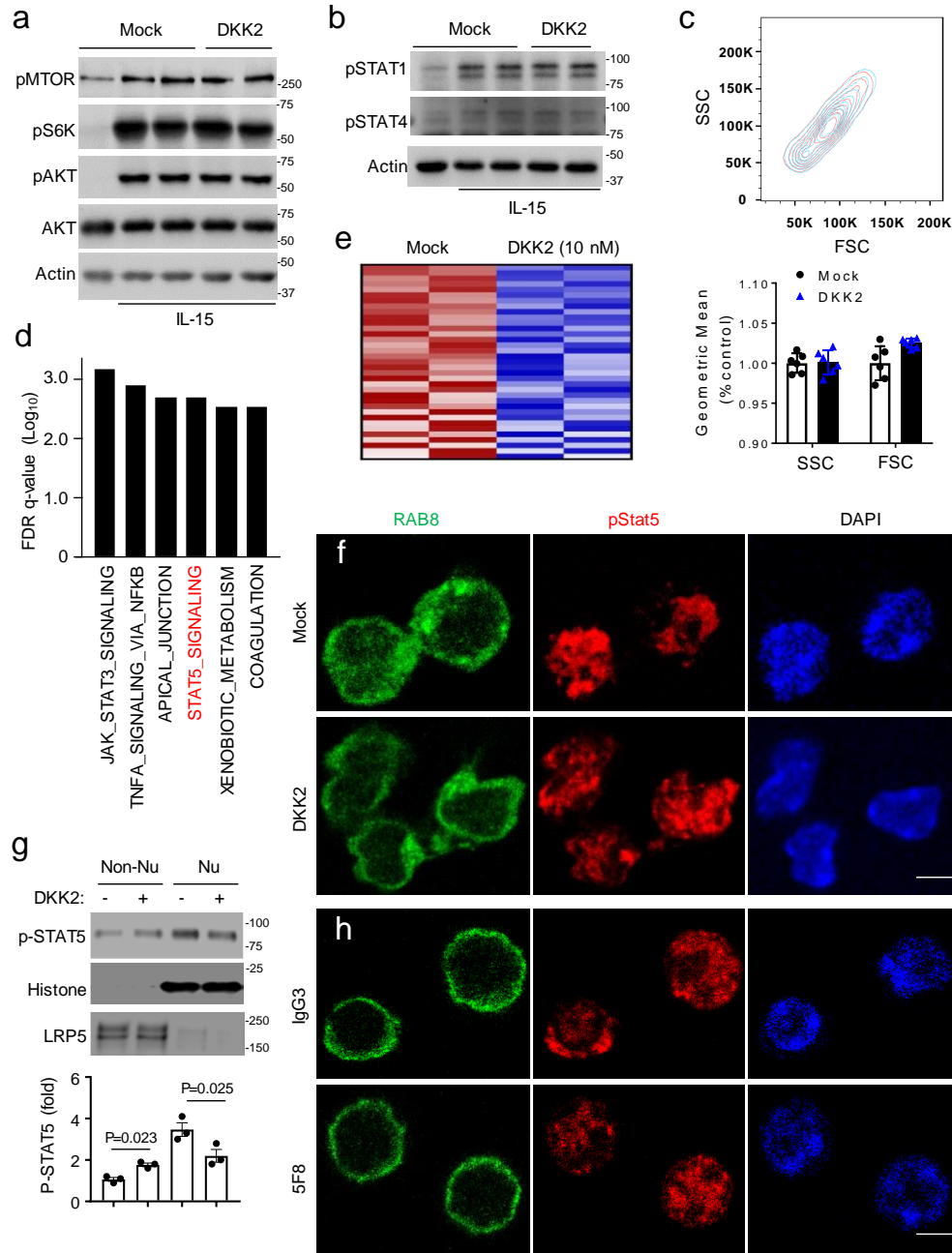
Supplementary Figure 5. Cytotoxic immune cell depletion. (a-c) Confirmation of cell depletion efficiencies by flow analysis for Fig. 3i and j. (d) Effects of CD8⁺ or NK1.1⁺ depletion on polyp formation in the *Apc^{min/+}* mice. Data are presented as means±sem (ns, not significant; n=6, two-way Anova for left panel; n=5, two-sided Student t-Test for right panel).



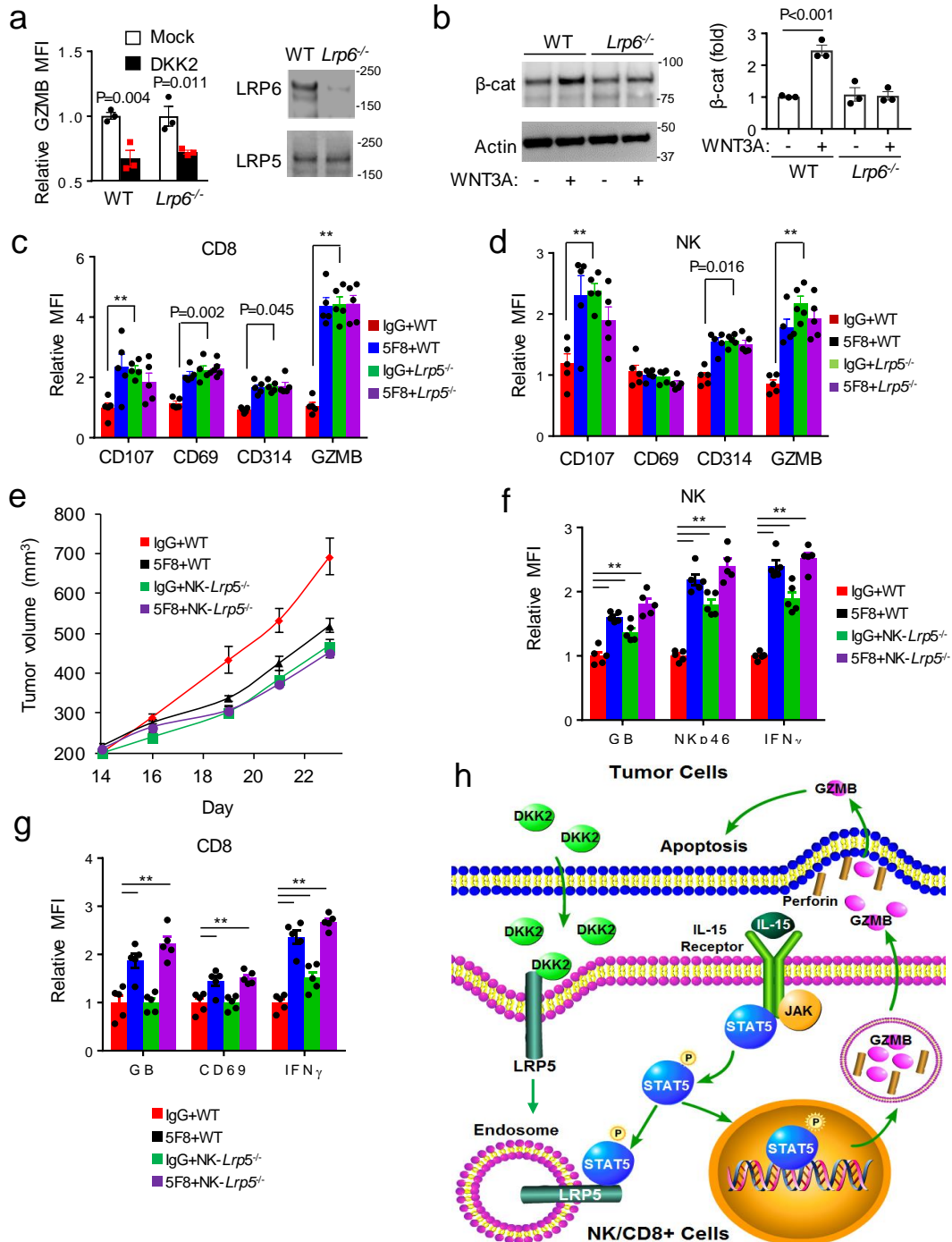
Supplementary Figure 6. DKK2 directly suppresses NK cell activation. **(a)** Reversal of DKK2-mediated inhibition of mouse NK cells by 5F8. NK cells were treated and analyzed as in Fig. 4d in the presence or absence of 36 μ g 5F8 or IgG3. Data are presented as means \pm sem (**, p <0.001 vs IgG or DKK2+5F8; n =5 except for IFN γ n =3; two-way Anova). **(b)** DKK2 inhibits mouse NK cells stimulated with IL12 and IL-18. Mouse primary NK cells were cultured with IL-12 and IL-18 (50 ng/ml) for 24 hrs. DKK2 protein (400 ng/ml) were then added for another 24 hours, followed by flow cytometry analyses. Data are presented as means \pm sem (** p <0.001 vs Mock+IgG or DKK2+5F8; n =3; Two-way Anova). The experiments were repeated twice. **(c)** DKK2 inhibits human NK cells. Human NK cells were isolated from peripheral bloods pooled from multiple normal individuals and incubated with human IL-15 (50 ng/ml) with or without 400 ng/ml human DKK2 protein for 24 hours before analysis by flow cytometry. Data are presented as means \pm sem (n =3; two-way Anova). The experiments were repeated three times. **(d)** DKK2 inhibits IL-15-mediated activation of mouse and human primary CD8 $^+$ T cells. Primary mouse CD8 $^+$ cells were isolated from spleens, whereas human CD8 $^+$ cells were isolated from peripheral blood using negative selection. These cells were cultured in IL-15 + IL15R α -Fc (50 ng/ml) for 4 days. DKK2 (400 ng/ml) was then added for 24 hours before flow analysis. Data are presented as means \pm sem (n =3; two-way Anova). The experiments were repeated two times. **(e)** DKK2 inhibits mouse IECs. Mouse IECs were isolated from normal mouse intestines and incubated with IL-15 (200 ng/ml) with or without 400 ng/ml DKK2 protein for 24 hours before analysis by flow cytometry. Data are presented as means \pm sem (n =3; Two-sided Student's t-test). The experiments were repeated twice.



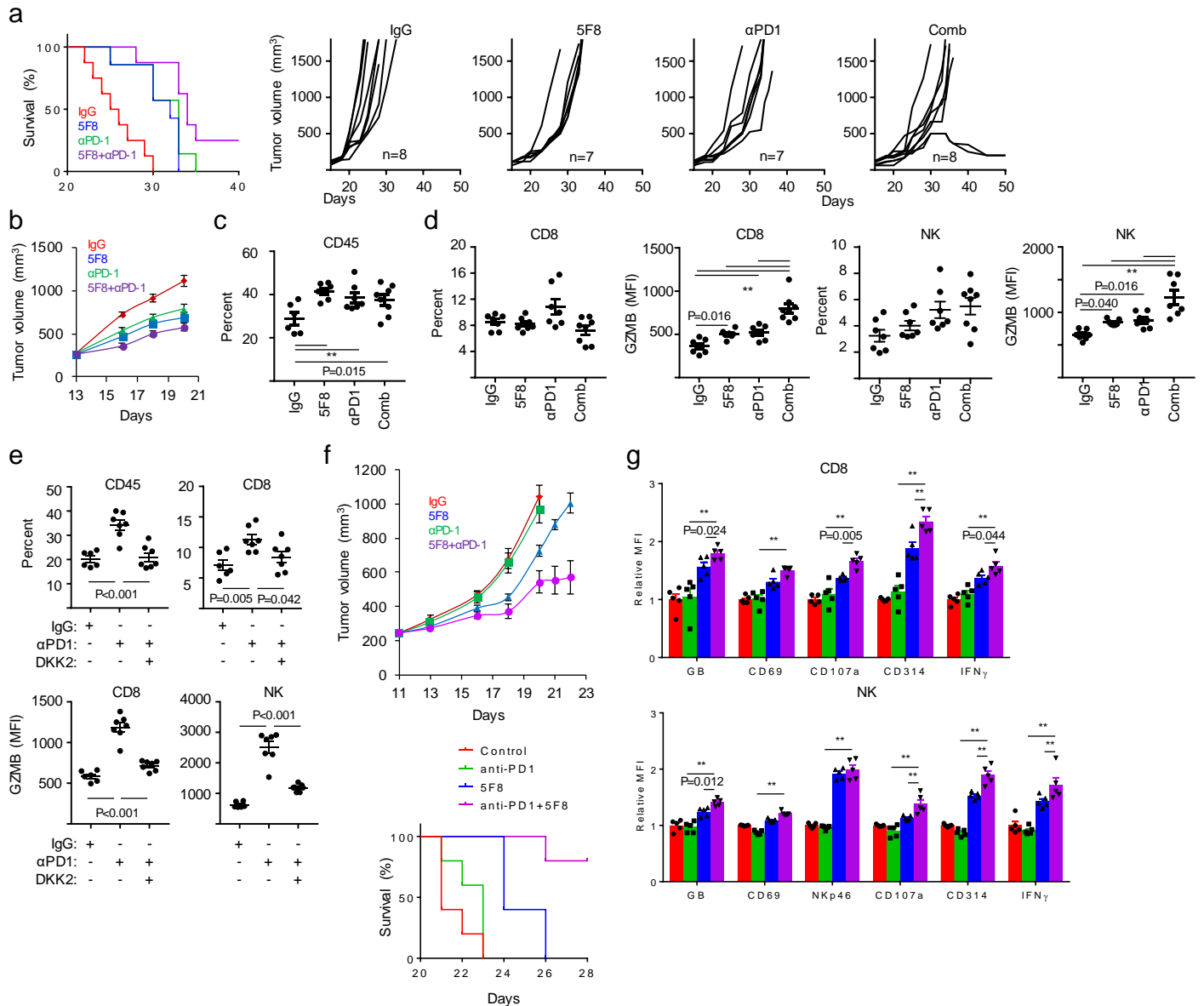
Supplementary Figure 7. DKK2 acts independently of Wnt-β-catenin signaling. (a) Wnt reporter gene assay. DKK2 (400 ng/ml), and Wnt3a (100 ng/ml), and GSK3 inhibitor CHIR (1 μM) were added for 6 hrs to cells transfected with TOPFLASH the day before as indicated. Data are presented as means±sem (Two-way Anova; n=3). The experiments were repeated twice. **(b)** LRP5-deficiency does not affect WNT3A-induced accumulation of β-catenin in primary mouse NK cells. Isolated primary mouse NK cells were expanded with IL-15 (50 ng/ml) for 24 hrs and then incubated with WNT3A (100 ng/ml) for 24 hours and analyzed by Western. The β-catenin blots were quantified and are shown as means±sem (two-way Anova, n=3). The experiments were repeated twice.



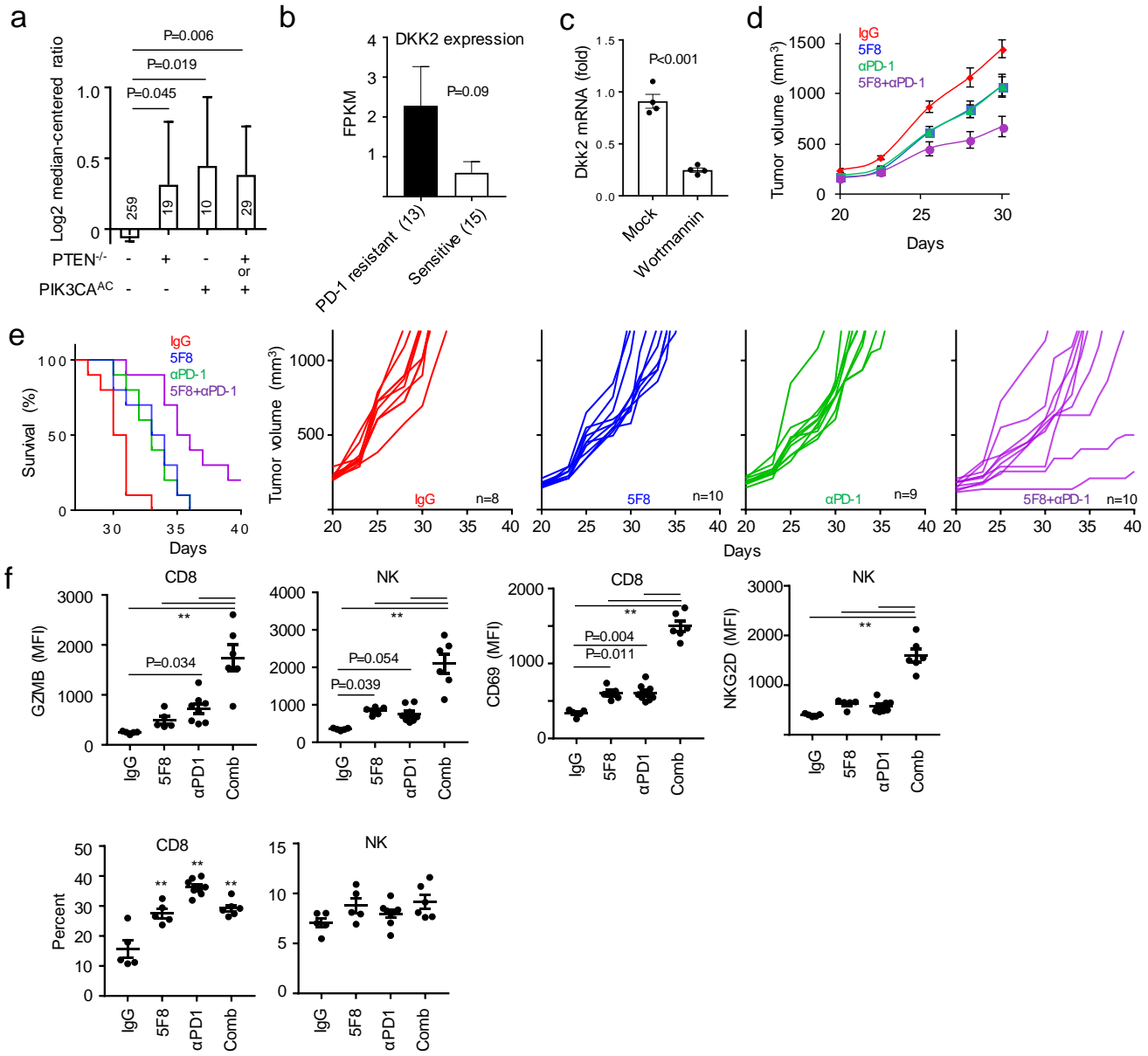
Supplementary Figure 8. DKK2 impedes phospho-STAT5 nuclear localization. (a-c) DKK2 does not affect the MTORC1 pathway, phosphorylation of STAT1 or STAT4, or cell size. NK cells were prepared and analyzed as in Fig. 5a. The experiments were repeated twice. (d-e) Analysis of RNA sequencing results reveals relationship of DKK2-treatment to STAT signaling in mouse NK cells. Mouse NK cells were prepared and treated as Fig. 4d, and mRNAs isolated from these NK cells were subjected to NGS. Panel d shows pathway enrichment, whereas Panel e shows alterations in expression of STAT5 motif genes. Gene names are listed in Supplementary Table I. (f,h) Individual channels for Figure 5b and c. (g) DKK2 alters distribution of p-STAT5. NK cells were treated as in Fig. 5a and subjected to subcellular fractionation. The Nuclear (Nu) and non-nuclear (Non-Nu; cytosolic and membrane fraction pool) fractions were analyzed by Western blotting. The p-STAT5 blots were quantified and are shown as means±sem (Two-sided Student's t-test, n=3).



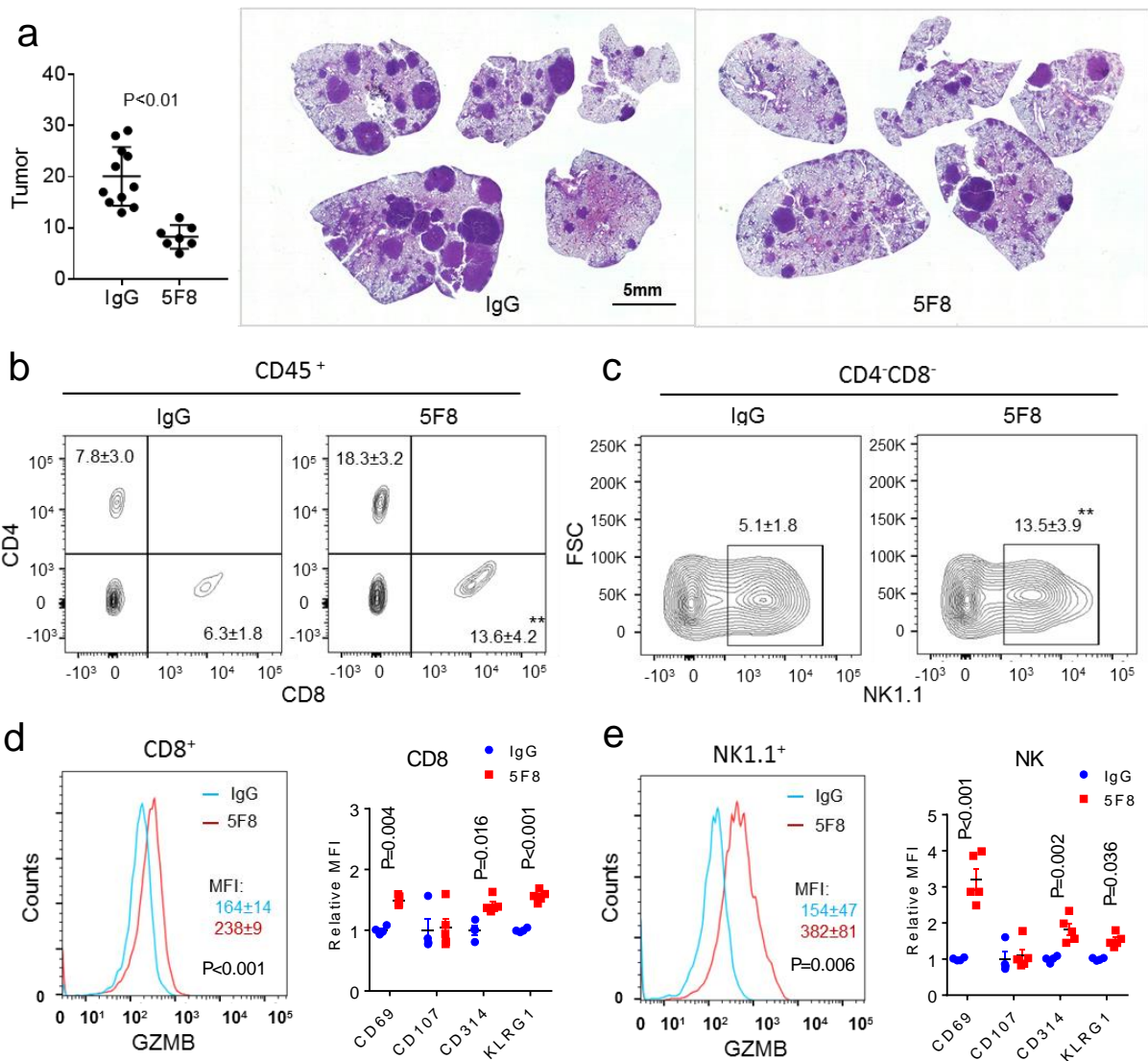
Supplementary Figure 9. DKK2 suppresses NK cells via LRP5, but not LRP6. (a) LRP6 is not required for DKK2-mediated inhibition of NK activation. Primary mouse NK cells were prepared from WT and $Lrp6^{-/-}$ mice and treated as Fig. 6a, followed by flow cytometry and Western analysis. Data are presented as means \pm sem ($n=3$; two-way Anova). The experiments were repeated twice. (b) LRP6 is required for WNT3A-induced stabilization of β -catenin in NK cells. Mouse NK cells were treated as in Supplementary Fig. 7b. The β -catenin blots were quantified and are shown as means \pm sd (Two-way Anova, $n=3$). (c,d) Flow cytometry analyses of infiltrated leukocytes in tumors described in Fig. 6c. Data are presented as means \pm sem (**, $p<0.001$; $n=5$; two-way Anova). (e-g) LRP5 in NK cells has a significant role in DKK2 blockade-mediated tumor suppression and NK cell activation. NK-specific knockout mice were generated by transferring bone marrows of WT or NCR1-Cre $Lrp5^{fl/fl}$ mice into WT recipient mice, followed with inoculation of MC38 cells. Treatment of 5F8 (10 mg/kg, i.p.) was given at Day 14, 19, and 22, followed by flow cytometry. Data are presented as means \pm sem ($P=0.002$ IgG+WT vs 5F8+WT in e; **, $p<0.001$; $n=5$ in f; two-way Anova). (h) A model for DKK2 to impart tumor immune evasion. DKK2 produced by tumor cells and possibly tumor infiltrated stromal cells binds to LRP5 on NK cells, leading to sequestration of phospho-STAT5 to endosomes and reduction in its nuclear localization. This in turn leads to an impediment in NK cell activation including a reduction in granzyme B production and attenuated NK-mediated tumor cell killing.



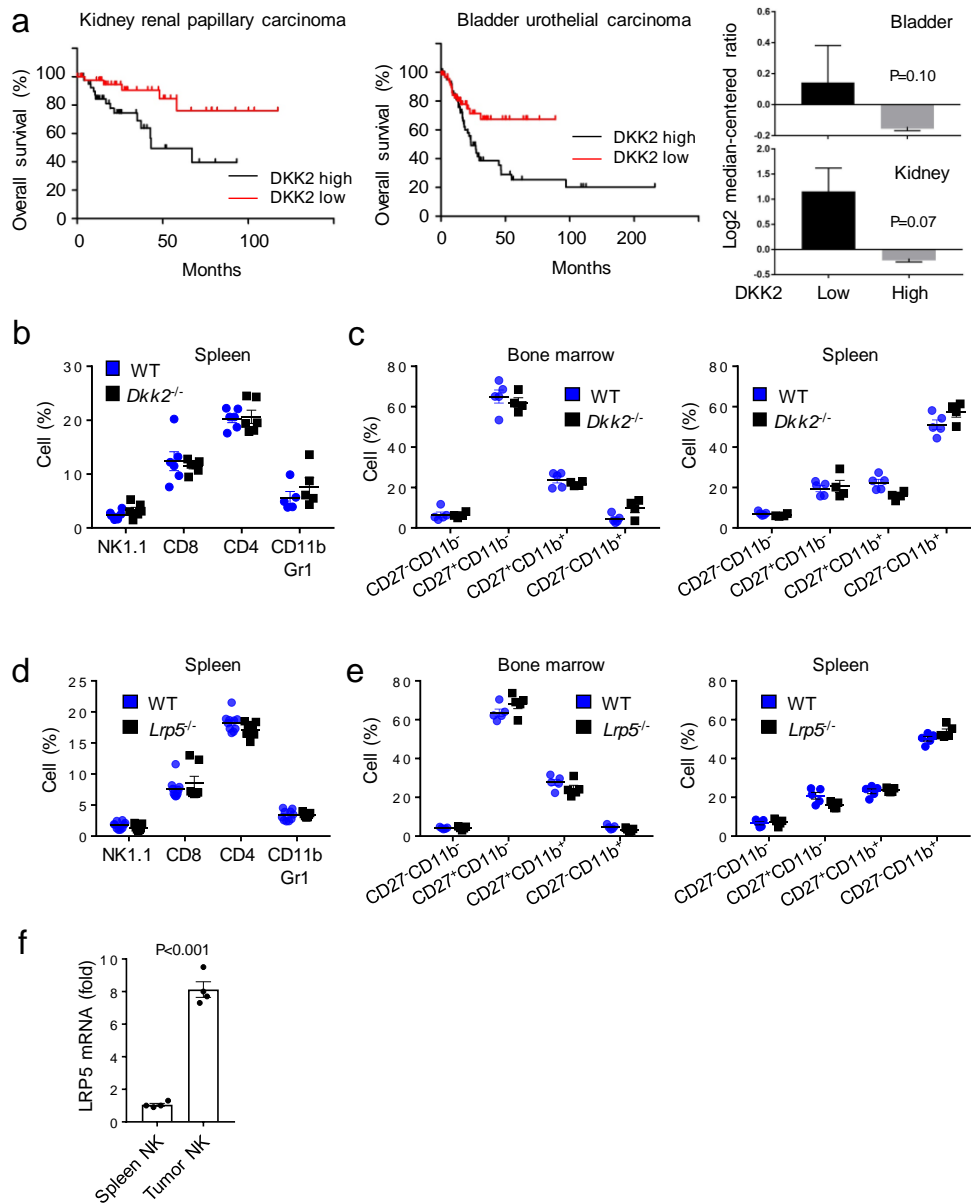
Supplementary Figure 10. DKK2 suppresses responses elicited by PD-1 blockade. (a) Augmented anti-tumor effects of DKK2 and PD-1 blockade combination in the MC38 tumor model. C57BL/6 mice were inoculated s.c. with MC38 cells. Treatment of IgG (20 mg/kg, n=8), 5F8+IgG (n=7), anti-PD-1+IgG (n=7), and 5F8+anti-PD-1 (n=8) (10 mg/kg each) in 100 μ l was done at every 5 days starting Day 18. Survival was evaluated by the two-sided Log-rank (Mantel-Cox) multiple comparison test with Bonferroni correction ($P < 0.001$, IgG vs combo; $P = 0.003$, IgG vs 5F8, $P = 0.003$ IgG vs α PD-1; $P = 0.082$, combo vs anti-PD-1; $P < 0.012$, combo vs 5F8). (b-d) Effects of the antibody treatments on cytotoxic immune cells. 57BL/6 mice were inoculated s.c. with the MC38 cells. Treatments of 5F8 and/or anti-PD-1 (10 mg/kg, i.p) were done at Days 13 and 18. Tumors were collected for flow cytometry analysis on Day 20. Tumor growth data are presented as means \pm sem ($P = 0.025$, IgG vs anti-PD-1; $P = 0.008$, IgG vs 5F8; $P < 0.001$ IgG vs combo for Day 20). Flow data are presented as means \pm sem (** $p < 0.01$; two-way Anova). (e) Effect of recombinant DKK2 protein on cytotoxic immune cell responses to PD-1 blockade. C57BL/6 mice were inoculated s.c. with the MC38 cell. When tumors grew to 500 mm³, they were injected with DKK2 protein (600 ng/25 μ l/tumor; multiple injection sites per tumor) for three times every 8 hours. One hour after the last inject, tumors were collected, and infiltrated leukocytes were analyzed by flow cytometry. Data are presented as means \pm sem (n=7; one-way Anova). (f) DKK2 blockade impedes progression of APC-loss MC38 tumors. C57BL/6 mice were inoculated s.c. with the APC mutant MC38 cells. Treatment of control IgG (20 mg/Kg), 5F8+IgG, anti-PD-1+IgG or 5F8+anti-PD-1 (10 mg/kg each) was done at Days 11, 16 and Day 20. Tumor growth data are presented as means \pm sem ($P = 0.016$, IgG vs 5F8, two-way Anova for Day 20; $P < 0.001$, 5F8 vs combo, Student's t-test for Day 23; n=5). Survival was evaluated by the two-sided Log-rank (Mantel-Cox) multiple comparison test with Bonferroni correction ($p = 0.002$, IgG vs 5F8 or combo; $p = 0.003$, anti-PD-1 vs 5F8 or combo; $p = 0.008$, 5F8 vs combo). (g) Effects of DKK2 blockade on immune effector cell activation in APC mutant MC38 tumors. The tumor implantation and antibody treatments were done as in f, but at Day 11 and 16. Tumors were collected at Day 18 and analyzed by flow cytometry. Data are presented as means \pm sem (**, $p < 0.001$; Two-way Anova; n=5).



Supplementary Figure 11. Effects of DKK2 and PD-1 combination blockade on a mouse melanoma tumor model. (a) Upregulation of DKK2 in human melanomas containing PTEN-loss and/or PI3K activated mutations. The numbers in the chart denote the sample size. (b) A trend of correlation between DKK2 expression upregulation and resistance to anti-PD-1 treatment in human melanomas. (c) PI3K inhibitor Wortmannin reduces DKK2 expression in YUMM1.7 cells. The cells were treated with Wortmannin (5 μ M) for 24 hours and DKK2 mRNA levels were determined by qRT-PCR. Data are presented as means \pm sem (Two-sided Student's t-test; n=4). The experiment was repeated three times. (d,e) Anti-tumor effects of DKK2 and PD-1 blockades in the YUMM1.7 tumor model. C57BL/6 mice were inoculated s.c. with the YUMM1.7 cells. Treatment of 5F8 and/or anti-PD-1 (10 mg/kg, i.p.) was done at every 5 days starting Day 12. Survival was evaluated by the two-sided Log-rank (Mantel-Cox) multiple comparison test with Bonferroni correction (p<0.001, IgG vs combo; p=0.004, IgG vs 5F8, p=0.003 IgG vs α PD-1, p=0.018 combo vs 5F8, p=0.007 Combo vs α PD-1). Mean tumor growth data are presented as means \pm sem (P values for Day 30 are: <0.001, IgG vs combo; 0.045, IgG vs 5F8 or α PD-1; 0.023, combo vs 5F8; 0.025, combo vs α PD-1; two-way Anova). (f) Effects of antibody treatments on cytotoxic immune cells on YUMM tumors in the 57BL/6 mice. Treatments of 5F8 and/or anti-PD-1 were done at Days 16 and 20. Tumors were collected for flow cytometry analysis on Day 21. Data are presented as means \pm sem (**, p<0.01; Two-way Anova).



Supplementary Figure 12. Anti-DKK2 antibody suppresses tumor progress and activate immune effector cells in lungs of *Apc^{fl/fl}Kras^{act/+}* mice. The mice (9 weeks old) were instilled intra-nasally with 65 ul of MEM containing adenovirus expressing Cre (2×10^7 plaque-forming unites) and CaCl_2 . After 6 weeks, the mice were treated weekly with IgG3 or 5F8 (10 mg/Kg). After another 6 weeks, the lungs ($n=10$ IgG and $n=7$ 5F8) were perfused and the number of tumors visible at the surfaces are shown in **a** (Data are presented as means±sem; two-sided Student's t-test). Some of the lungs are sectioned, and five histological sections from a lung of a representative IgG or 5F8-treated lung are also shown in **a**. The rest of the lungs were analyzed by flow cytometry (**b-e**). Data are presented as means±sem (**, $p < 0.001$ vs IgG; $n=5$; Two-sided Student's t-test).



Supplementary Figure 13. Augmented anti-tumor effects of DKK2 and PD-1 combination blockade. (a) Correlations between DKK2 expression and cancer patient survival rates and granzyme B expression. The survival rates of the high (top 15 percentile) and low (bottom 15 percentile) DKK2 expressers are compared using the TCGA provisional datasets of kidney renal papillary carcinoma (P=0.006; n=43) and bladder urothelial carcinoma (P=0.012; n=61) by the two-sided Mantel-Cox Log-Rank test. Trends of correlation of DKK2 expression with granzyme B are also noted. **(b,d)** DKK2- or LRP5-deficiency does not alter the NK1.1⁺, CD8⁺, CD4⁺, or CD11b⁺Gr1 population in spleens. Mice of 8 weeks old female were used. Data are presented as mean±sem (n=5). **(c,e)** DKK2- or LRP5-deficiency does not alter NK cell developments. Mice of 8 weeks old female were used. Data are presented as mean±sem (n=5). Cells are pre-gated for the CD3^{e-} CD19⁻ NK1.1⁺ population. **(f)** Upregulation of LRP5 mRNA in tumor infiltrated NK cells. RNA was isolated from NK cells sorted from MC38 grafted tumors and primary NK cells from spleen and analyzed by qRT-PCR. Data are presented as mean±sem (n=4; two-sided Student t-test).

Supplementary Figure 14. Uncropped Western blots

Figure 5a

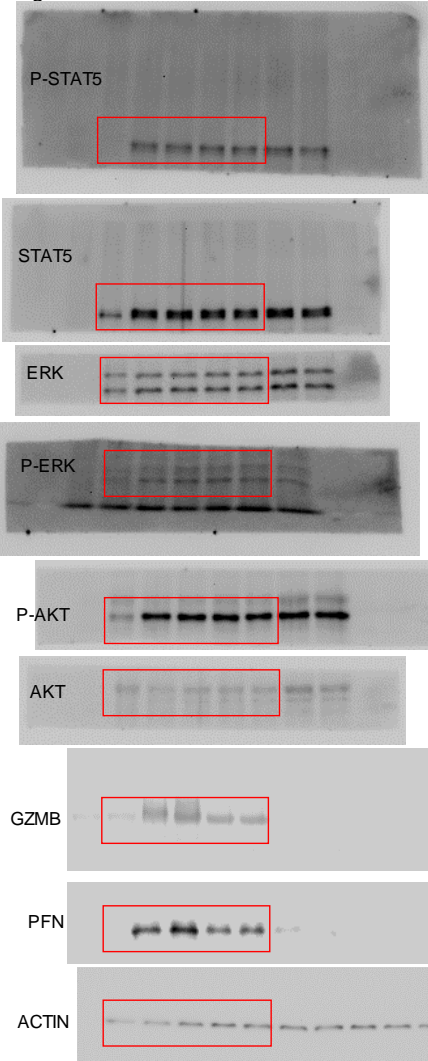


Figure 6a

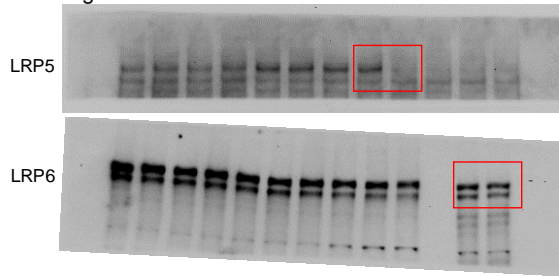


Figure 6d

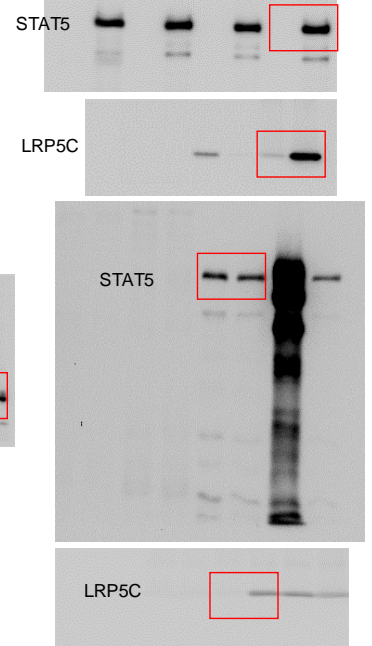


Figure 6f

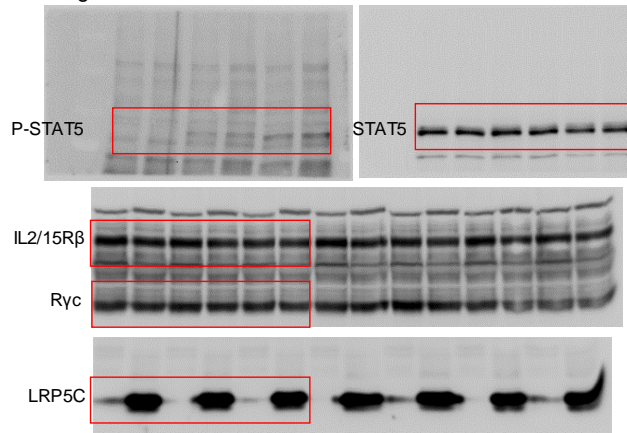


Figure 6i

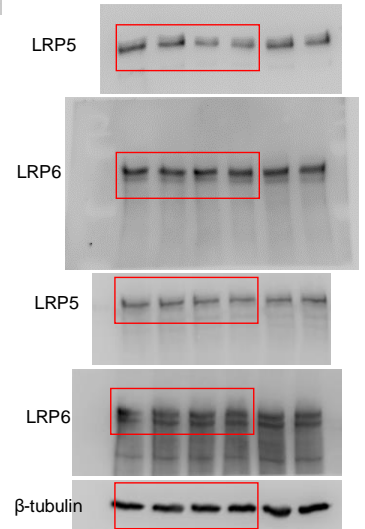
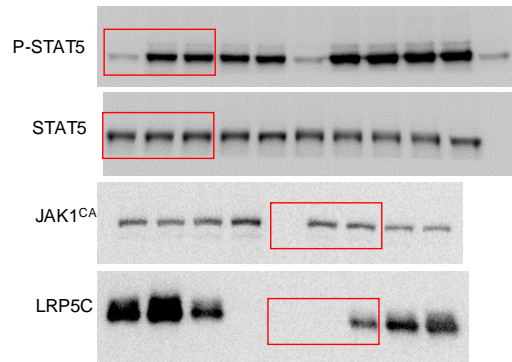
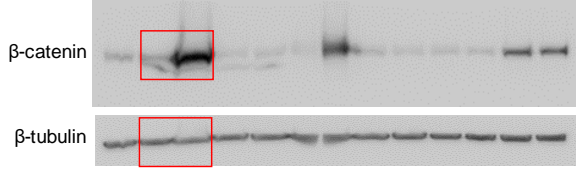


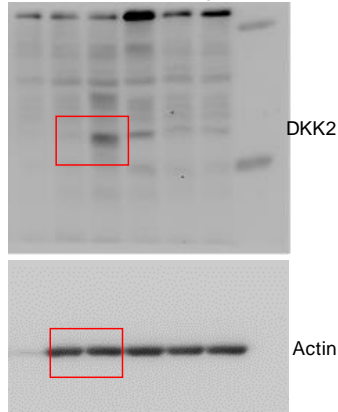
Figure 6g



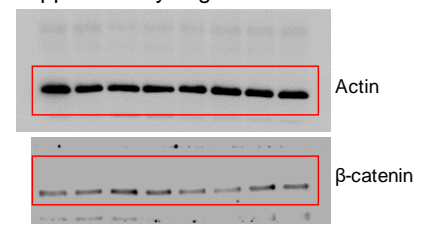
Supplementary Figure 1e



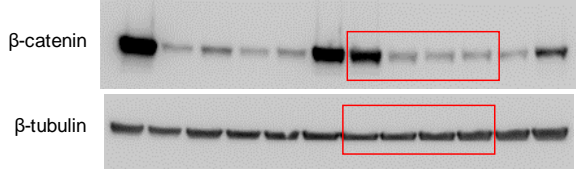
Supplementary Figure 11



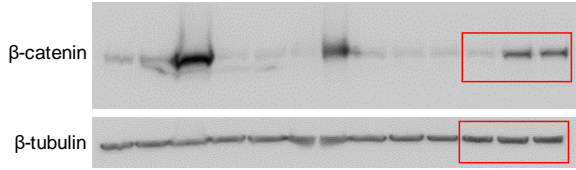
Supplementary Figure 7b



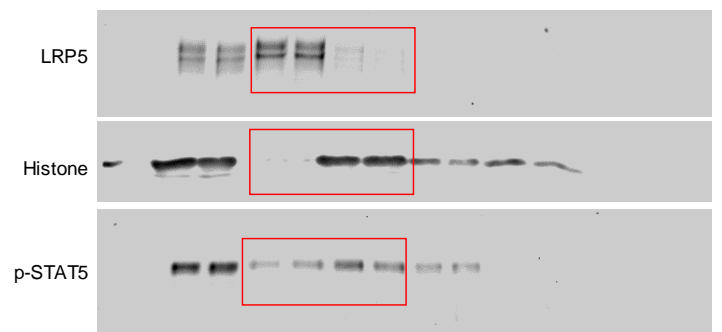
Supplementary Figure 1f



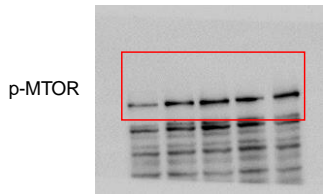
Supplementary Figure 1g



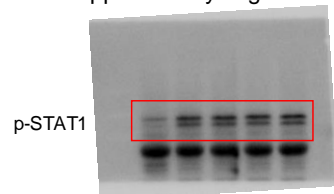
Supplementary Figure 8g



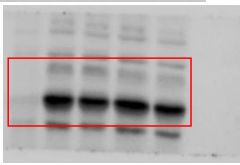
Supplementary Figure 8a



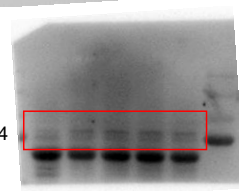
Supplementary Figure 8b



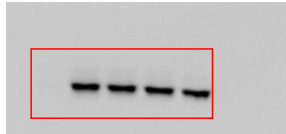
p-S6K



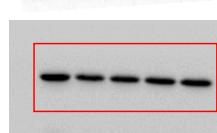
p-STAT4



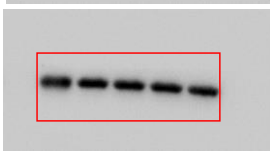
p-AKT



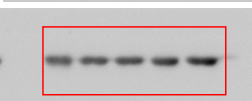
Actin



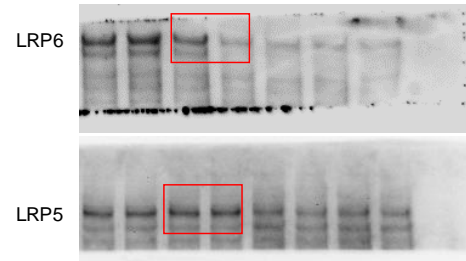
AKT



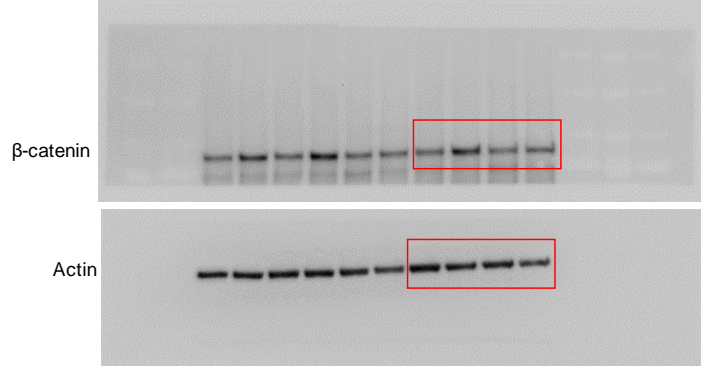
Actin



Supplementary Figure 9a



Supplementary Figure 9b



Supplementary Table I_STAT5 regulated genes

Gene symbol	1.Control	2.Control	1.DKK2	2.DKK2
DACH2	1.134291418	0.837028498	-0.7989581	-1.17236182
ATP2A2	1.125646644	0.843963719	-1.18600457	-0.7836058
TRAF6	0.707956444	1.245124141	-1.12007019	-0.83301039
GABPA	0.795629313	1.145082364	-0.67660469	-1.26410698
CPSF7	0.61789126	1.317507259	-1.03662422	-0.8987743
LIF	1.267547989	0.666072892	-1.16709042	-0.76653046
KBTBD8	1.311749802	0.611822649	-0.79607561	-1.12749684
CXADR	0.961553377	0.960529814	-0.57014795	-1.35193524
RYBP	1.110673586	0.811190912	-1.32258949	-0.59927501
GZMB	1.327468792	0.586402749	-0.78015019	-1.13372135
MTF2	1.356238161	0.555187192	-0.84254954	-1.06887582
MBNL3	0.819714839	1.074392976	-1.38290085	-0.51120697
MBNL1	1.406649866	0.478676452	-0.85612604	-1.02920028
CNOT2	0.728268669	1.147095489	-1.38226127	-0.49310288
PHF17	0.494819716	1.377503379	-0.70720631	-1.16511679
ATP11C	0.635351836	1.231913801	-0.52413559	-1.34313004
SMC1A	0.900380767	0.962219247	-1.44550288	-0.41709713
FZD6	1.156898099	0.703866253	-1.39671741	-0.46404694
RUNX1	1.34830992	0.474703147	-1.29558267	-0.52743039
ELMO1	1.045394847	0.772946974	-1.48211031	-0.33623152
TMEM163	1.447204212	0.368095023	-1.15508685	-0.66021239
SPRED1	0.316037626	1.479245294	-0.67355086	-1.12173206
PURA	0.559594139	1.235114653	-0.37254187	-1.42216692
SPRY4	1.496913016	0.293910016	-0.70920631	-1.08161672
CMTM6	1.44587472	0.34237932	-1.20500999	-0.58324405
ZBTB20	1.175749257	0.599404997	-1.47184634	-0.30330792
AKAP1	0.268512591	1.502859469	-1.10977856	-0.6615935
PTCH1	1.480121654	0.219832553	-1.24746382	-0.45249038
ANKRD28	0.252777962	1.445609037	-0.3997168	-1.2986702
HMGN5	0.293850769	1.389849125	-0.31055508	-1.37314481
WIPF1	1.251465807	0.429709726	-1.48711978	-0.19405575
PPP2R3A	0.253338693	1.427711392	-0.3483386	-1.33271149
Prf1	1.450652674	0.195478548	-1.3243245	-0.32180672
OPN3	0.148401627	1.426873165	-0.19549527	-1.37977952
LCOR	0.115537556	1.410049502	-1.40882121	-0.11676585

Supplementary Table II_Primer sequences

qRT Primers

hDKK2	CGACACACCATGCAGGCCGA
hDKK2	CCTGGTCAGGCCGCAATCG
mDKK2	TCAACTCCATCAAGTCCTCTC
mDKK2	TCACATTCCTTATCACTGCTG

SiRNA sequences

	Mixed (GUGAAAUUCUUGGCUAUUA; GCGCUUGGCUGAACCAUCA; AAGCUGACCUGAUGGAGUU;
siCTNNB1-1	CAGCAAUUAUGCGCCUUU)
siCTNNB1-2	GUGAAAUUCUUGGCUAUUA
siCTNNB1-3	GCGCUUGGCUGAACCAUCA

SgRNA guiding sequences

Cas9 mAPC-1F	CACCGTTGGAGAGAGCGAGGTAT
Cas9 mAPC-1R	AAACatacctcgctctctctcaaC
Cas9 mAPC-2F	CACCGTGCCACACAATGGAACCTCGG
Cas9 mAPC-2R	AAACccgagttcattgtgtggcaC
hAPC 855aa Cas9-1F1	CACCGTTGGAGAGAGAACGCGGAAT
hAPC 855aa Cas9-1R1	AAACattccgcttctctctcaaC
hAPC 900aa cas9-1F2	CACCGGTCTTCCTGAGAGGTATGAA
hAPC 900aa cas9-1R2	AAACttcacctctcaggaagacC
hAPC 1345aa cas9-2F1	CACCGGTTTATCTTCAGAATCAGCC
hAPC 1345aa cas9-2R1	AAACggctgattctgaagataaacC
hAPC 1385AA cas9-2F2	CACCGTACATCTGCTAAACATGAGT
hAPC 1385AA cas9-2R2	AAACactcatgttagcagatgtaC